

The Milky Way revealed to be a neutrino desert by the IceCube Galactic plane observation

Received: 21 March 2023

Ke Fang¹✉, John S. Gallagher^{2,3} & Francis Halzen¹

Accepted: 13 October 2023

Published online: 27 November 2023

 Check for updates

The Galactic diffuse emission (GDE) is formed when cosmic rays leave the sources where they were accelerated, diffusively propagate in the Galactic magnetic field and interact with the interstellar medium and interstellar radiation field. GDE in γ -rays (GDE- γ) has been observed up to subpetaelectronvolt energies, although its origin may be explained by either cosmic-ray nuclei or electrons. Here we show that the γ -rays accompanying the high-energy neutrinos recently observed by the IceCube Observatory from the Galactic plane have a flux that is consistent with the GDE- γ observed by the Fermi-LAT and Tibet AS γ experiments around 1 TeV and 0.5 PeV, respectively. The consistency suggests that the diffuse γ -ray emission above \sim 1 TeV could be dominated by hadronuclear interactions, although a partial leptonic contribution cannot be excluded. Moreover, by comparing the fluxes of the Galactic and extragalactic diffuse emission backgrounds, we find that the neutrino luminosity of the Milky Way is one-to-two orders of magnitude lower than the average of distant galaxies. This finding implies that our Galaxy has not hosted the type of neutrino emitters that dominates the isotropic neutrino background at least in the past few tens of kiloyears.

High-energy neutrinos have been observed from the Milky Way by the IceCube Observatory between 0.5 TeV and multi-petaelectronvolts^{1,2}. The Galactic diffuse emission (GDE) in neutrinos (GDE- ν) is identified at a 4.5σ significance using cascade data and templates describing the diffuse flux of photons. Unresolved individual sources also potentially contribute to the observed events. Less than \sim 10 TeV, the GDE flux measured using the π^0 model, based on the megaelectronvolt-to-gigaelectronvolt π^0 component measured by the Fermi-Large Area Telescope (LAT)³, and the CRINGE model⁴, based on a global fit of cosmic rays, is higher than that using the KRA models⁵, which implement radially dependent cosmic-ray diffusion. Although the π^0 and CRINGE models are slightly favoured by the data, the preference is not statistically significant².

The Galactic diffuse emission in γ -rays (GDE- γ) has been measured by Fermi-LAT from 100 MeV to 1 TeV (ref. 3). Above \sim 1 TeV, GDE- γ has been observed by ground-based γ -ray experiments from the parts

of the Galactic plane that are accessible to the detectors^{6,7}. The GDE- γ above 100 TeV has been detected by the Tibet Air Shower gamma-ray experiment (Tibet AS γ)⁸, The High-Altitude Water Cherenkov Observatory (HAWC)⁷ and the Large High Altitude Air Shower Observatory (LHAASO)'s square km array (KM2A)(LHAASO-KM2A)⁹ observatories. Most of the photons observed by Tibet AS γ with energy above 398 TeV do not point to known γ -ray sources, suggesting that the emission could be diffuse in nature. By contrast, LHAASO-KM2A finds a lower GDE intensity for a similar sky region when masking known and new sources detected by LHAASO⁹. This hints at the postulation that the Tibet AS γ flux could partly be contributed by unresolved sources¹⁰.

GDE may come from protons and nuclei when they interact with gas in the interstellar medium (ISM). Diffuse γ -ray emission may also be produced by the inverse Compton radiation of relativistic electrons. The fraction of leptonic contribution to the GDE- γ is still under debate.

¹Department of Physics, Wisconsin IceCube Particle Astrophysics Center, University of Wisconsin, Madison, WI, USA. ²Department of Astronomy, University of Wisconsin, Madison, WI, USA. ³Department of Physics and Astronomy, Macalester College, St Paul, MN, USA.

✉e-mail: kefang@physics.wisc.edu

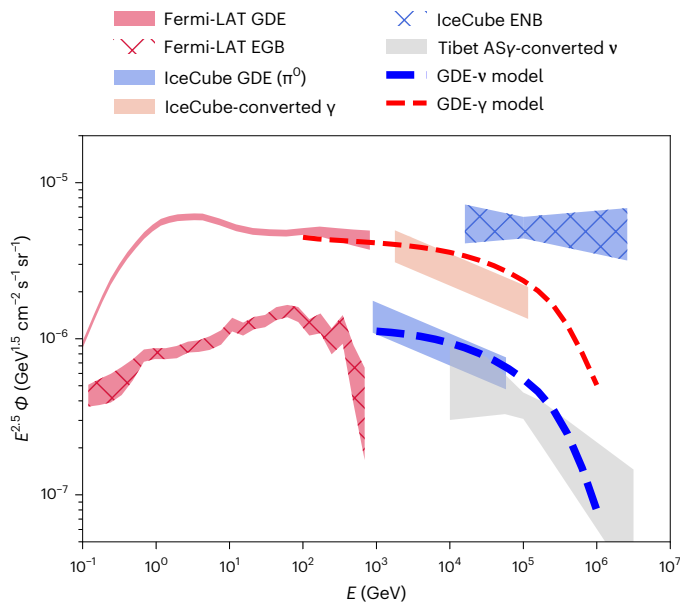


Fig. 1 | All-sky-averaged intensities of the Galactic diffuse emission (GDE) and extragalactic background (EB) in γ -ray and neutrinos. The intensity has been scaled by $E^{2.5}$. Galactic components include the diffuse neutrino emission (per-flavour flux including both neutrinos and antineutrinos) from the Galactic plane measured by IceCube using the π^0 template¹ (blue-shaded region indicating the 1σ uncertainties), the neutrino flux derived from the GDE- γ measured by Tibet AS γ ^{8,18} (grey-shaded region) and the Galactic interstellar emission model of Fermi-LAT²⁰ (red-shaded region). The dashed curves present a numerical simulation of the diffuse emission that accounts for the spatial distribution of sources and gas in the Milky Way. Extragalactic components include the isotropic diffuse neutrino background measured by IceCube³⁶ (blue-hatched region) and the EGB measured by Fermi-LAT³⁰ (red-hatched region).

Copious inverse Compton radiation has been suggested to come from the Galactic bulge and inner Galaxy, contributing to both around a few gigaelectronvolts and above 10 TeV (refs. 11,12). A hardening in the diffuse γ -ray spectrum at 0.1–1 TeV, sometimes referred to as the ‘TeV excess’, has been interpreted as a signature of unresolved TeV halos owing to electrons trapped around middle-aged pulsars¹³ or pulsar wind nebulae¹⁴, or as a result of a progressive hardening of cosmic-ray nuclei spectra towards the Galactic Centre owing to effects such as the anisotropic cosmic-ray transport¹⁵.

Cosmic-ray protons and nuclei interact with the ISM gas and produce neutrinos and γ -rays simultaneously via $\pi^\pm \rightarrow e^\pm \nu_e(\bar{\nu}_e) \bar{\nu}_\mu \nu_\mu$ and $\pi^0 \rightarrow 2\gamma$. The flux of the γ -rays that accompany the IceCube Galactic diffuse neutrinos can be estimated by $E_\nu^2(dN_{inj}/dE_\nu) \approx 2/3E_\nu^2(dN/dE_\nu)$, with $E_\nu \approx 2E_\nu$ (ref. 16). Here dN_{inj}/dE_ν denotes the injected γ -ray spectrum, which could be different from the observed γ -ray spectrum owing to the pair production of γ -rays on low-energy photons. Photons above ~ 100 TeV may be absorbed by the interstellar radiation field, whereas the attenuation effect is negligible for lower-energy photons^{17,18}. As shown in Fig. 1, the γ -ray flux derived from the IceCube measurement is comparable to the Fermi-LAT Galactic interstellar emission model around 1 TeV (note that both the terms ‘interstellar γ -ray emission’ and ‘Galactic diffuse emission’ refer to the diffuse emission made by energetic cosmic rays interacting with interstellar nucleons and photons¹⁹). The model is obtained by fitting various templates of the diffuse γ -ray emission and models of resolved and unresolved sources to the Fermi-LAT data between 100 MeV and 1 TeV (ref. 20). The systematic error in the effective area of Fermi-LAT Pass 8 data is estimated to be 5% between 0.1 GeV and 100 GeV and 15% at 1 TeV with a linear interpolation in the logarithm of energy between 100 GeV and 1 TeV. We used the systematic error to estimate the uncertainty of the Galactic interstellar

emission spectrum. The actual measurement error may also arise from the model uncertainties and the separation of the isotropic emission¹⁹ and thus be higher than the systematics of the detector.

The flux of the GDE- ν observed by IceCube is also consistent with that of the diffuse neutrinos expected to accompany the subpetaelectronvolt diffuse γ -rays observed by Tibet AS γ . The silver-shaded region in Fig. 1, from ref. 18, is an estimation of the Galactic plane emission derived from the Tibet AS γ measurements in two sky regions, namely, region A: $25^\circ < l < 100^\circ$ and region B: $50^\circ < l < 200^\circ$, both with $|b| < 5^\circ$. The width of the band accounts for the uncertainties owing to the spectra and spatial distribution of cosmic rays, gas density and infrared emission of the ISM. The IceCube observation between 10 TeV and ~ 60 TeV agrees with this Tibet-converted neutrino flux within the uncertainties.

The consistency in the GDE measurements by Fermi-LAT, Tibet AS γ and IceCube at various energies suggests that the GDE- γ could be dominantly produced by hadronic interaction above ~ 1 TeV. However, given the uncertainty of the GDE- ν flux associated with the analysis templates and the potential contribution from unresolved neutrino sources, leptonic processes may still have a role in particular between 0.1 TeV and a few teraelectronvolts.

Subsequently, we consider a GDE model under the assumption that the IceCube flux based on the π^0 template represents the diffuse neutrino flux and the source contribution is negligible. The modelling of diffuse neutrino and γ -ray emission is impacted by several poorly known factors, including (1) cosmic-ray spectra above the rigidity ~ 10 TV observed at Earth; (2) the difference in the cosmic-ray density at a location \mathbf{x} in the Galaxy and that at the observer point, $n(\mathbf{x}, E)/n(r_\odot, E)$, which is determined by the source distribution in the Galaxy, timescales of the sources and the particle diffusion in the Galactic magnetic field; and (3) the density profile of the neutral, ionized and dark gas. The effects of these factors could be coupled and are not constrained by current observations, as also noted by, for example, refs. 4,12,21,22.

To limit the degrees of freedom of our model, as in refs. 17,23,24, we consider a simplified model in which the spatial and spectral components of the nucleon flux are assumed to be independent, $\Phi(\mathbf{x}, E) = \Phi(\mathbf{x}_\odot, E) [n(\mathbf{x})/n(\mathbf{x}_\odot)]$. We obtain the ratio of cosmic-ray density at position \mathbf{x} to that at the solar neighbourhood, $n(\mathbf{x})/n(\mathbf{x}_\odot)$, using a numerical simulation that propagates cosmic rays from synthetic sources in the Galactic magnetic field. We fix the spectra of protons and helium nuclei at the solar neighbourhood, $\Phi(\mathbf{x}_\odot, E)$, to the best-fit model obtained by fitting to the cosmic-ray measurements between ~ 10 GeV and ~ 10 PeV. More details about the simulation and the calculation of the intensity of neutrino and γ -ray emission are explained in Supplementary Sections 1 and 2, respectively.

The dashed curves in Fig. 1 from our model show that the hadronic interaction may simultaneously explain the observed γ -ray spectra between 100 GeV and 100 TeV and the diffuse neutrino flux of the Galactic plane measured using the π^0 template. More complicated models including multiple components of cosmic-ray sources and diffusion regions^{4,21} may provide better fits to the data. Future measurements of longitudinal and latitudinal profiles of neutrino emission above 1 TeV, identification of individual Galactic neutrino sources and observation of GDE- γ from the southern sky at teraelectronvolt–petaelectronvolt energies are needed to break down the degeneracy of the model parameters.

The GDE flux reflects the emissivity of our own Galaxy in high-energy neutrinos, whereas the extragalactic background (EB) reveals the contribution of powerful sources in distant galaxies. Had the local and distant sources been similarly luminous, the GDE would be brighter than the EB owing to geometry. Figure 1 contrasts the intensities of the GDE and EB in γ -ray and neutrinos. Notably, the all-sky-averaged GDE- γ is brighter than the extragalactic γ -ray background (EGB) between 1 GeV and 1 TeV, whereas the GDE- ν is fainter than the extragalactic neutrino background (ENB) between 1 TeV and

100 TeV. The fact suggests that the Milky Way in its current state is not a typical source of high-energy neutrinos.

The integrated differential flux at the neutrino energy E_ν observed today from galaxies extending to cosmic ‘high noon’ (at redshift $z \approx 2 - 3$) in which the star-formation rate peaks can be calculated as:

$$E_\nu^2 \Phi_\nu^{\text{EG}}(E_\nu) = \frac{c}{4\pi} \int_0^{z_{\text{max}}} dz \left| \frac{dt}{dz} \right| \frac{1}{1+z} \int_{M_{\text{min}}}^{M_{\text{max}}} dM \frac{dn}{dM}(M, z) L_\nu^{\text{EG}}(E_\nu, M, z), \quad (1)$$

in which $E'_\nu = E_\nu(1+z)$ is the energy of a neutrino at redshift z , $|dt/dz| = (H_0(1+z)\sqrt{\Omega_M(1+z)^3 + \Omega_\Lambda})^{-1}$ with $H_0 = 67.4 \text{ km s}^{-1} \text{ Mpc}^{-1}$, $\Omega_M = 0.315$ and assuming a flat universe²⁵, $L_\nu^{\text{EG}}(E'_\nu, M, z) \equiv E_\nu'^2 d\dot{N}_\nu/dE'_\nu(M, z)$ is the neutrino luminosity of an external galaxy. The number density n of galaxies with stellar mass M at redshift z is $dn/dM(M, z)$ given by the Schechter²⁶ function, $dn/d\log M = \phi^* \ln(10)(10^{\log M - \log M^*})^{\alpha+1} \exp(-10^{\log M - \log M^*})$. The normalization ϕ^* , slope α and characteristic mass M^* are found by fitting the mass function to galaxy distribution at different redshift bins up to $z \approx 3$ (refs. 27–29).

We assume that the neutrino emissivity of a galaxy, including contributions from both the individual sources hosted by the Galaxy and the Galactic diffuse emission, is related to the stellar mass and redshift independently:

$$L_\nu^{\text{EG}}(E'_\nu, M, z) = L_\nu^{\text{EG}}(E'_\nu, M_{\text{MW}}, 0) \left(\frac{M}{M_{\text{MW}}} \right)^\beta g(z)(1+z)^{2-s}. \quad (2)$$

In equation (2), we have parameterized the dependence of the stellar mass as a power law with an index β depending on source models. In an extreme scenario in which all galaxies are equally luminous, $\beta = 0$. In a more realistic scenario in which the neutrino luminosity scales to the optical, near-infrared or X-ray luminosity of galaxies, one would expect $\beta \approx 1$ (refs. 30,31). The γ -ray luminosities of the star-forming galaxies detected by Fermi-LAT present a relation of $L_\gamma \propto L_{\text{IR}}^{1.35}$ (ref. 32). If the neutrino luminosity is proportional to the bolometric luminosity of the AGN, then β may reach as high as 1.47 (ref. 33). Without specifying the neutrino source types, subsequently we float β from 0 to 2.0.

The function $g(z)$ in equation (2) describes the source evolution over redshift. In a uniform evolution scenario, $g(z) = 1$. If the sources follow a star-formation history, $g(z)$ can be modelled as $g(z) \propto (1+z)^{3.4}$ at $z < 1$, $(1+z)^{-0.3}$ at $1 < z < 4$ and $(1+z)^{-3.5}$ at $z > 4$ (ref. 34). A star-formation model with higher redshift contributions enhances the integrated flux by a factor of order unity. Our calculation considers both the uniform and star-formation models.

The last term in equation (2) arises from the fact that a neutrino observed at E_ν today was at the energy $E_\nu(1+z)$ at the source. So $E_\nu'^2 dN_\nu/dE'_\nu \propto (1+z)^{2-s}$ when assuming that the neutrino spectrum follows a non-broken power law $dN_\nu/dE'_\nu \propto E_\nu'^{-s}$. Measurements of the diffuse isotropic neutrino flux find the index $s \approx 2.5$ between -1 TeV and a few petaelectronvolts^{35–37}. Without loss of generality, we take $s = 2.0 - 3.0$.

As explained in Methods, the all-sky-averaged intensity of the GDE observed at the solar neighbourhood may be related to the total neutrino power of the Milky Way through $E_\nu^2 \Phi_\nu^{\text{MW}}(E_\nu) = F_e(E_\nu)(3/4\pi)(L_\nu^{\text{MW}}(E_\nu)/4\pi r_\odot^2)$, with $r_\odot \approx 8.5 \text{ kpc}$ being our distance to the Galactic Centre and F_e a geometry factor of the order unity that accounts for the profiles of gas and sources.

Equations (1) and (2) may also apply to γ -rays when the attenuation owing to $\gamma\gamma$ pair production with the cosmic-microwave background and the interstellar radiation field is negligible, which is the case below -100 GeV. Note that equation (2) makes no assumption on the production mechanism of the γ -rays and thus holds true regardless of their hadronic or leptonic origin. When deriving the total luminosity of

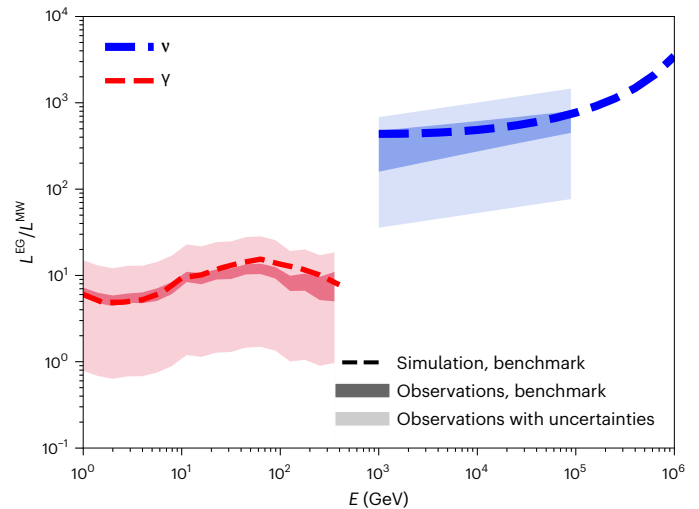


Fig. 2 | Derived ratio of the average luminosity of an external, Milky Way-like Galaxy and the Galactic luminosity in giga-electronvolt–tera-electronvolt γ -rays and tera-electronvolt–peta-electronvolt neutrinos. γ -rays are shown in red; neutrinos are shown in blue. The ratio is calculated using equations (1), (2), (4) and (5) with the Fermi-LAT and IceCube measurements of the GDE. The dark-shaded regions adopt the benchmark extragalactic model parameters and assume a uniform emissivity within the Galactic disk. Their widths correspond to the uncertainties in the GDE and EB observations. The dashed curves use not only the benchmark extragalactic model but also a more realistic Galactic model that takes into account the spatial distribution of sources and gas in the Milky Way. The light-shaded region further accounts for the uncertainties in the parameters of the extragalactic model.

the Milky Way using the GDE, we have assumed that the contribution of resolved and unresolved sources in the Galaxy is negligible. This is consistent with the observation of Fermi-LAT up to -100 GeV (refs. 3,19).

The ratio of the luminosities of an external, Milky Way-like Galaxy to the Milky Way, $L^{\text{EG}}/L^{\text{MW}} \equiv L^{\text{EG}}(M_{\text{MW}}, 0)/L^{\text{MW}}$, in neutrinos can be estimated as:

$$\frac{L_\nu^{\text{EG}}}{L_\nu^{\text{MW}}} \approx \frac{\Phi_\nu^{\text{EG}}}{\Phi_\nu^{\text{MW}}} \frac{3F_e}{4\pi r_\odot^2 n_0 c t_H \xi_z} = 120 \left(\frac{\Phi_\nu^{\text{EG}}/\Phi_\nu^{\text{MW}}}{5} \right) \left(\frac{n_0}{0.01 \text{ Mpc}^{-3}} \right)^{-1} \left(\frac{\xi_z}{3} \right)^{-1} \left(\frac{F_e}{1} \right), \quad (3)$$

in which n_0 is the local density of galaxies with a stellar mass similar to that of the Milky Way and the quantity ξ_z accounts for the evolution of the source emissivity over cosmic time³⁸. ξ_z is determined by $g(z)$ and varies from -0.5 for uniform evolution to -3 for star-formation evolution. Although the analytical expression in equation (3) demonstrates the dependence on various parameters, the extragalactic–Galactic ratio presented subsequently is numerically computed using equations (1), (2), (4) and (5).

Figure 2 presents $L^{\text{EG}}/L^{\text{MW}}$ derived from tera-electronvolt–peta-electronvolt neutrino and giga-electronvolt–tera-electronvolt γ -ray observations. For the extragalactic diffuse background, we take $\beta = 1$, $s = 2.5$ and $g(z)$, following the star-formation history as the benchmark model. The dark-shaded regions show the results obtained with the extragalactic benchmark model and by assuming a uniform γ -ray and neutrino emissivity ($\epsilon_{\nu,\gamma}$ in equation (5)) inside the Galactic plane. The widths of the dark-shaded region are propagated errors from the observational uncertainties of the ENB measured with the IceCube 6-year cascade events³⁶, the GDE- ν flux found by IceCube with the π^0 diffusion template¹ and the EGB measured by Fermi-LAT assuming foreground model A³⁹. For comparison, the dashed curve shows the ratio derived with the same extragalactic model parameters but with a more realistic

GDE model from the simulation. The light-shaded region additionally accounts for the uncertainties in the parameters β , s and $g(z)$. In all cases, we find that L_V^{EG} is not significantly different from L_V^{MW} but $L_V^{EG}/L_V^{MW} \gg 1$. In other words, the Milky Way at the present time is an atypical neutrino emitter. The IceCube observation of the GDE confines this ratio to $\sim 30\text{--}10^3$, depending on the neutrino energy. Our finding also suggests that giga-electronvolt γ -rays are suppressed relative to the neutrinos observed by IceCube. Giga-electronvolt γ -rays are either barely produced in the process in which tera-electronvolt neutrinos are generated or the accompanying γ -rays are attenuated by the radiation field at the neutrino production site.

Our result suggests that the Galaxy has not hosted the type of emitters that dominate the ENB in the past $D/c \approx 26$ kyr ($D/8$ kpc), which is the time taken by a neutrino to travel from a Galactic source at a kpc-scale distance D to the Earth. Cosmic rays at tera-electronvolt–peta-electronvolt energy are confined by the Galactic magnetic field for million-year durations⁴⁰. Had any major cosmic-ray sources injected protons into the ISM within that time period, the diffuse neutrino flux of the Galactic plane would be higher and the gap in the neutrino luminosity of our Galaxy and an external Milky Way-like Galaxy would be smaller.

There is compelling evidence for a highly energetic Seyfert explosion from the supermassive black hole at the Galactic Centre a few million years in the past. Among that, the clearest indications are the Fermi and eROSITA bubbles^{41,42}. The time to the last burst/flare is constrained to 2–10 Myr by both the mechanical timescales needed to explain the morphology and multiwavelength spectra of the observed bubbles and haze⁴³ and kinematic studies of halo gas^{44–46}. In addition, elevated ionizing radiation along the Magellanic Stream⁴⁷ independently constrains this nuclear activity. These timescales are consistent with the scenario in which most peta-electronvolt protons from the last jet activity have already left the Galaxy today and the Milky Way is no longer an active neutrino emitter. Other sources or mechanisms that are not present or extremely rare in the Milky Way over the past tens of thousands of years, such as tidal disruption events, could also contribute to the ENB. These sources are probably γ -ray-obscured as suggested by both the observations of the isotropic neutrino flux^{48,49} and individual neutrino sources⁵⁰.

Methods

Neutrino emissivity and intensity of the Galaxy

The all-sky-averaged intensity of the Galactic plane observed at the solar neighbourhood is

$$E_\nu^2 \Phi_\nu^{MW}(E_\nu) = \frac{1}{4\pi} \int_{-\pi/2}^{\pi/2} \cos(b) db \int_0^{2\pi} dl I_\nu(l, b, E_\nu), \quad (4)$$

in which $I_\nu(l, b, E_\nu) = (1/4\pi) \int_0^\infty ds \epsilon_\nu(l, b, r, E_\nu)$ is the intensity from the direction with Galactic longitude and latitude (l, b) along a line of sight s of the observer, and $\epsilon_\nu(l, b, r, E_\nu)$ is the production rate of neutrinos per unit volume in units of $\text{eV s}^{-1} \text{cm}^{-3}$ at a distance r from the Galactic Centre, which is related to the total neutrino power emitted by the Milky Way, L_V^{MW} , through

$$L_V^{MW}(E_\nu) = \int_{-\pi/2}^{\pi/2} \cos(b) db \int_0^{2\pi} dl \int_0^\infty r^2 dr \epsilon_\nu(l, b, r, E_\nu). \quad (5)$$

Unresolved point-like and extended sources may contribute to both the Tibet AS γ and IceCube observations^{1,8}. Equations (4) and (5) still apply in the presence of individual sources. Similar to equations (1) and (2), these two equations may also apply to γ -rays when the γ -ray absorption by the interstellar radiation field is negligible.

The intensity of the Galactic plane depends on the emission profile. We can rewrite equations (4) and (5) as $E_\nu^2 \Phi_\nu^{MW}(E_\nu) = F_\epsilon(E_\nu)(3/4\pi)(L_V^{MW}(E_\nu)/4\pi r_0^2)$, with F_ϵ denoting a geometry factor of the order unity that accounts for the profiles of gas and sources. It

essentially states that the total flux of the GDE observed at the solar neighbourhood is, to the first order, comparable to the flux from a point source at the Galactic Centre that carries the power of the entire Galaxy. When assuming that ϵ_ν is independent of E_ν and uniform in the Galactic disk as in the leaky box model, with the disk defined as $R_d < 15$ kpc and $z_d < 0.2$ kpc, we obtain $F_\epsilon = 1.16$. Alternatively, we find $F_\epsilon = 0.97$ when assuming that ϵ_ν follows the spatial distribution of supernova remnants¹⁸.

Data availability

Source data for Fig. 1 are available online. Any additional data are available from the corresponding author upon reasonable request.

Code availability

The calculation used publicly available software packages including HERMES (<https://github.com/cosmicrays/hermes>) and CRPropa (<https://github.com/CRPropa>).

References

- IceCube Collaboration. Observation of high-energy neutrinos from the Galactic plane. *Science* **380**, 1338–1343 (2023).
- Fuerst, P. M. et al. Galactic and extragalactic analysis of the astrophysical muon neutrino flux with 12.3 years of IceCube Track Data. *Proc. Sci. ICRC2023*, 1046 (2023).
- Ackermann, M. et al. Fermi-LAT observations of the diffuse gamma-ray emission: implications for cosmic rays and the interstellar medium. *Astrophys. J.* **750**, 3 (2012).
- Schwefer, G., Mertsch, P. & Wiebusch, C. Diffuse emission of Galactic high-energy neutrinos from a global fit of cosmic rays. *Astrophys. J.* **949**, 16 (2023).
- Gaggero, D., Grasso, D., Marinelli, A., Urbano, A. & Valli, M. The gamma-ray and neutrino sky: a consistent picture of Fermi-LAT, Milagro, and IceCube results. *Astrophys. J. Lett.* **815**, L25 (2015).
- Abramowski, A. et al. Diffuse Galactic gamma-ray emission with H.E.S.S. *Phys. Rev. D* **90**, 122007 (2014).
- Abeysekara, A. U. et al. Galactic gamma-ray diffuse emission at TeV energies with HAWC data. *Proc. Sci. ICRC2021*, 835 (2021).
- Tibet AS γ Collaboration et al. First detection of sub-PeV diffuse gamma rays from the Galactic disk: evidence for ubiquitous Galactic cosmic rays beyond PeV energies. *Phys. Rev. Lett.* **126**, 141101 (2021).
- Cao, Z. et al. Measurement of ultra-high-energy diffuse gamma-ray emission of the Galactic plane from 10 TeV to 1 PeV with LHAASO-KM2A. *Phys. Rev. Lett.* **131**, 151001 (2023).
- Vecchiotti, V., Zuccarini, F., Villante, F. L. & Pagliaroli, G. Unresolved sources naturally contribute to PeV gamma-ray diffuse emission observed by Tibet AS γ . *Astrophys. J.* **928**, 19 (2022).
- Porter, T. A., Jóhannesson, G. & Moskalenko, I. V. High-energy gamma rays from the Milky Way: three-dimensional spatial models for the cosmic-ray and radiation field densities in the interstellar medium. *Astrophys. J.* **846**, 67 (2017).
- Porter, T. A., Jóhannesson, G. & Moskalenko, I. V. The GALPROP Cosmic-ray Propagation and Nonthermal Emissions Framework: Release v57. *Astrophys. J. Suppl. Ser.* **262**, 30 (2022).
- Linden, T. & Buckman, B. J. Pulsar TeV halos explain the diffuse TeV excess observed by Milagro. *Phys. Rev. Lett.* **120**, 121101 (2018).
- Vecchiotti, V., Pagliaroli, G. & Villante, F. L. The contribution of Galactic TeV pulsar wind nebulae to Fermi large area telescope diffuse emission. *Commun. Phys.* **5**, 161 (2022).
- Cerri, S. S., Gaggero, D., Vittino, A., Evoli, C. & Grasso, D. A signature of anisotropic cosmic-ray transport in the gamma-ray sky. *J. Cosmol. Astropart. Phys.* **2017**, 019 (2017).

16. Ahlers, M. & Murase, K. Probing the Galactic origin of the IceCube excess with gamma-rays. *Phys. Rev.* **D90**, 023010 (2014).
17. Lipari, P. & Vernetto, S. Diffuse Galactic gamma-ray flux at very high energy. *Phys. Rev. D* **98**, 043003 (2018).
18. Fang, K. & Murase, K. Multimessenger implications of sub-PeV diffuse Galactic gamma-ray emission. *Astrophys. J.* **919**, 93 (2021).
19. Acero, F. et al. Development of the model of Galactic interstellar emission for standard point-source analysis of Fermi large area telescope data. *Astrophys. J. Suppl. Ser.* **223**, 26 (2016).
20. Abdollahi, S. et al. Fermi Large Area Telescope fourth source catalog. *Astrophys. J. Suppl. Ser.* **247**, 33 (2020).
21. Evoli, C. et al. Cosmic-ray propagation with DRAGON2: I. Numerical solver and astrophysical ingredients. *J. Cosmol. Astropart. Phys.* **2017**, 015 (2017).
22. De La Torre Luque, P. et al. Galactic diffuse gamma rays meet the PeV frontier. *Astron. Astrophys.* **672**, A58 (2023).
23. Pagliaroli, G., Evoli, C. & Villante, F. L. Expectations for high energy diffuse Galactic neutrinos for different cosmic ray distributions. *J. Cosmol. Astropart. Phys.* **2016**, 004 (2016).
24. Cataldo, M., Pagliaroli, G., Vecchiotti, V. & Villante, F. L. Probing Galactic cosmic ray distribution with TeV gamma-ray sky. *J. Cosmol. Astropart. Phys.* **2019**, 050 (2019).
25. Planck Collaboration et al. Planck 2018 results. VI. Cosmological parameters. *Astron. Astrophys.* **641**, A6 (2020).
26. Schechter, P. An analytic expression for the luminosity function for galaxies. *Astrophys. J.* **203**, 297–306 (1976).
27. Fasano, G. et al. WINGS: a wide-field nearby galaxy-cluster survey. I. Optical imaging. *Astron. Astrophys.* **445**, 805–817 (2006).
28. Tomczak, A. R. et al. Galaxy stellar mass functions from ZFOURGE/CANDELS: an excess of low-mass galaxies since $z = 2$ and the rapid buildup of quiescent galaxies. *Astrophys. J.* **783**, 85 (2014).
29. Conselice, C. J., Wilkinson, A., Duncan, K. & Mortlock, A. The evolution of galaxy number density at $z < 8$ and its implications. *Astrophys. J.* **830**, 83 (2016).
30. Bell, E. F., McIntosh, D. H., Katz, N. & Weinberg, M. D. The optical and near-infrared properties of galaxies. I. Luminosity and stellar mass functions. *Astrophys. J. Suppl. Ser.* **149**, 289–312 (2003).
31. Gilfanov, M. Low-mass X-ray binaries as a stellar mass indicator for the host galaxy. *Mon. Not. R. Astron. Soc.* **349**, 146–168 (2004).
32. Kornecki, P. et al. γ -Ray/infrared luminosity correlation of star-forming galaxies. *Astron. Astrophys.* **641**, A147 (2020).
33. Suh, H. et al. No significant evolution of relations between black hole mass and galaxy total stellar mass up to $z = 2.5$. *Astrophys. J.* **889**, 32 (2020).
34. Hopkins, A. M. & Beacom, J. F. On the normalization of the cosmic star formation history. *Astrophys. J.* **651**, 142–154 (2006).
35. IceCube Collaboration et al. IceCube high-energy starting event sample: description and flux characterization with 7.5 years of data. *Phys. Rev. D* **104**, 022002 (2021).
36. Aartsen, M. G. et al. Characteristics of the diffuse astrophysical electron and tau neutrino flux with six years of IceCube high energy cascade data. *Phys. Rev. Lett.* **125**, 121104 (2020).
37. Abbasi, R. et al. Improved characterization of the astrophysical muon–neutrino flux with 9.5 years of IceCube Data. *Astrophys. J.* **928**, 50 (2022).
38. Waxman, E. & Bahcall, J. High energy neutrinos from astrophysical sources: an upper bound. *Phys. Rev. D* **59**, 023002 (1998).
39. Ackermann, M. et al. The spectrum of isotropic diffuse gamma-ray emission between 100 MeV and 820 GeV. *Astrophys. J.* **799**, 86 (2015).
40. Strong, A. W., Moskalenko, I. V. & Ptuskin, V. S. Cosmic-ray propagation and interactions in the Galaxy. *Annu. Rev. Nucl. Part. Sci.* **57**, 285–327 (2007).
41. Ackermann, M. et al. The spectrum and morphology of the Fermi bubbles. *Astrophys. J.* **793**, 64 (2014).
42. Predehl, P. et al. Detection of large-scale X-ray bubbles in the Milky Way halo. *Nature* **588**, 227–231 (2020).
43. Yang, H. Y. K., Ruzsowski, M. & Zweibel, E. G. Fermi and eROSITA bubbles as relics of the past activity of the Galaxy’s central black hole. *Nat. Astron.* **6**, 584–591 (2022).
44. Fox, A. J. et al. Probing the Fermi bubbles in ultraviolet absorption: a spectroscopic signature of the Milky Way’s biconical nuclear outflow. *Astrophys. J. Lett.* **799**, L7 (2015).
45. Miller, M. J. & Bregman, J. N. The interaction of the Fermi bubbles with the Milky Way’s hot gas halo. *Astrophys. J.* **829**, 9 (2016).
46. Bordoloi, R. et al. Mapping the nuclear outflow of the Milky Way: studying the kinematics and spatial extent of the northern Fermi bubble. *Astrophys. J.* **834**, 191 (2017).
47. Bland-Hawthorn, J. et al. The large-scale ionization cones in the Galaxy. *Astrophys. J.* **886**, 45 (2019).
48. Murase, K., Guetta, D. & Ahlers, M. Hidden cosmic-ray accelerators as an origin of TeV–PeV cosmic neutrinos. *Phys. Rev. Lett.* **116**, 071101 (2016).
49. Fang, K., Gallagher, J. S. & Halzen, F. The TeV diffuse cosmic neutrino spectrum and the nature of astrophysical neutrino sources. *Astrophys. J.* **933**, 190 (2022).
50. IceCube Collaboration et al. Evidence for neutrino emission from the nearby active galaxy NGC 1068. *Science* **378**, 538–543 (2022).

Acknowledgements

The work of K.F. and F.H. is supported by the Office of the Vice Chancellor for Research and Graduate Education at the University of Wisconsin-Madison with funding from the Wisconsin Alumni Research Foundation. K.F. acknowledges support from the National Science Foundation (PHY-2110821 and PHY-2238916) and NASA (NMF211ZDA001N-Fermi). This work was supported by a grant from the Simons Foundation (00001470, K.F.). J.S.G. thanks the University of Wisconsin College of Letters and Science for partial support of his IceCube-related research. The research of F.H. was also supported in part by the US National Science Foundation under grants PHY-2209445 and OPP-2042807.

Author contributions

K.F. carried out the simulations and analyses and prepared the paper. All authors participated in the interpretation of the results and edited the paper.

Competing interests

The authors declare no competing interests.

Additional information

Supplementary information The online version contains supplementary material available at <https://doi.org/10.1038/s41550-023-02128-0>.

Correspondence and requests for materials should be addressed to Ke Fang.

Peer review information *Nature Astronomy* thanks Luigi Tibaldo and the other, anonymous, reviewer(s) for their contribution to the peer review of this work.

Reprints and permissions information is available at www.nature.com/reprints.

Publisher's note Springer Nature remains neutral with regard to jurisdictional claims in published maps and institutional affiliations.

Open Access This article is licensed under a Creative Commons Attribution 4.0 International License, which permits use, sharing, adaptation, distribution and reproduction in any medium or format, as long as you give appropriate credit to the original author(s) and the source, provide a link to the Creative Commons license, and indicate if changes were made. The images or other third party material in this

article are included in the article's Creative Commons license, unless indicated otherwise in a credit line to the material. If material is not included in the article's Creative Commons license and your intended use is not permitted by statutory regulation or exceeds the permitted use, you will need to obtain permission directly from the copyright holder. To view a copy of this license, visit <http://creativecommons.org/licenses/by/4.0/>.

© The Author(s) 2023